COMMUNICATIONS

CATALYSIS
COMMUNICATIONS

Available online at www.sciencedirect.com

SciVerse ScienceDirect

Journal Homepage:
www.elsevier.com/locate/catcom

(This is a sample cover image for this issue. The actual cover is not yet available at this time.)

Short Communication

The effect of Fe on the catalytic performance of Rh–Mn–Li/SiO$_2$ catalyst: A DRIFTS study

Jun Yu [a,b], Dongsen Mao [b,*], Lupeng Han [b], Qiangsheng Guo [b], Guanzhong Lu [a,b,*]

[a] Research Institute of Industrial Catalysis, East China University of Science and Technology, Shanghai 200237, PR China
[b] Research Institute of Applied Catalysis, School of Chemical and Environmental Engineering, Shanghai Institute of Technology, Shanghai 201418, PR China

ARTICLE INFO

ABSTRACT

Different amounts of Fe promoted Rh–Mn–Li/SiO$_2$ catalysts were prepared and investigated for the synthesis of C$_2$ oxygenates from syngas. The results showed that the low amount of Fe ($\leq$0.1 wt.%) improved the reactivity and yield of C$_2^+$ oxygenates, but an opposite effect appeared at high content of Fe ($>$0.1 wt.%). Diffuse reflectance infrared Fourier transform spectroscopy was used to probe the effects of Fe on CO adsorption and hydrogenation, and two opposing effects were evidenced. Moreover, it is proposed that the facile transformation of dicarbonyl Rh$^+$(CO)$_2$ into H–Rh–CO is responsible for high selectivity of C$_2^+$ oxygenates.

© 2012 Elsevier B.V. All rights reserved.

1. Introduction

Catalytic transformations of syngas (CO + H$_2$), which can be produced from non-petroleum carbon resources including natural gas, coal, and biomass, into C$_2$ oxygenates (e.g., ethanol, acetaldehyde and acetic acid) have attracted much attention in recent years because of the desire to decrease the global dependence on petroleum [1–4].

So far, SiO$_2$-supported Rh-based catalysts have been proven to be the most efficient ones in this C$_2$ oxygenate synthesis process. However, in order to commercialize this process, continuous research has been done to enhance the catalytic performance of the catalysts [5–9]. Very recently, we found that the Rh–Mn–Li catalyst supported on a novel SiO$_2$ prepared by the Stöber method, exhibited higher activity and C$_2$ oxygenate selectivity compared with that on a commercial SiO$_2$ [10]. On the other band, Fe as a promoter has been investigated extensively, because of its interesting promoting effects on the performance of Rh-based catalysts for CO hydrogenation. In the early 1990s, Guglielminotti et al. [6] and Burch et al. [11] have already found that the addition of Fe could enhance the selectivity of C$_2$ oxygenates over Rh-based catalysts. Later, Yin et al. [7] reported that the yield of C$_2$ oxygenates over Rh–Mn–Li/SiO$_2$ catalyst increased when appropriate amount of Fe was added. Recently, Goodwin and co-workers [12–14] also confirmed the promoting effect of Fe on Rh-based/SiO$_2$ catalysts for CO hydrogenation. Based on the above results, it is considered that the Fe promoter can be tried to further

enhance the catalytic performance of Rh–Mn–Li catalyst supported on the SiO$_2$ prepared by the Stöber method.

Here, various amounts of Fe promoted Rh–Mn–Li/SiO$_2$ catalysts were prepared and tested for the C$_2$ oxygenate synthesis from syngas, aiming to improve the catalytic performance of Rh–Mn–Li/SiO$_2$ catalyst. Moreover, insights into the effect of Fe on Rh–Mn–Li/SiO$_2$ for CO hydrogenation were demonstrated by diffuse reflectance infrared Fourier transform spectroscopy (DRIFTS).

2. Experimental

2.1. Catalyst preparation

SiO$_2$ was prepared by the Stöber method as reported in Ref. [10]. Before used, it was calcined in static air at 350 °C for 4 h. Aqueous solutions of RhCl$_3$ hydrate (Rh~36 wt.%), Mn(NO$_3$)$_2$·6H$_2$O and Li$_2$CO$_3$ were co-impregnated on the SiO$_2$, dried overnight at 120 °C and calcined for 4 h at 350 °C (heating rate~3 °C/min). The Rh loading was 1.5 wt.% and the weight ratio of Rh:Mn:Li was 1.5:1.5:0.07. The weight percent of Fe was listed in related tables and figures.

2.2. CO hydrogenation

CO hydrogenation was performed in a fixed-bed micro-reactor with length of ~350 mm and internal diameter of ~5 mm. The catalyst (0.3 g) was diluted with inert α-alumina (1.2 g) to avoid channeling and hot spots. Prior to reaction, the fresh catalyst was heated to 400 °C (heating rate~3 °C/min) and reduced with 10% H$_2$/N$_2$ (total flow rate = 50 mL/min) for 2 h at atmospheric pressure. Then, the reactor was cooled to 300 °C and the reaction started at a space velocity

* Corresponding authors. Tel.: +86 21 6087 7221; fax: +86 21 6087 7231.
E-mail addresses: dsmao1106@yahoo.com.cn (D. Mao), gzhlu@ecust.edu.cn (G. Lu).

(S.V.) of 10,000 mL/(g·h) and pressure of 3 MPa. The feed gas contained 60% H_2, 30% CO and 10% N_2. All post-reactor lines and valves were heated to 150 °C to prevent product condensation. The products were analyzed on-line (Agilent GC 6820) using a HP-PLOT/Q column (30 m, 0.32 mm ID) with an FID (flame ionization detector) and a TDX-01 column with a TCD (thermal conductivity detector). The CO conversion was calculated based on the fraction of CO that formed carbon-containing products and the selectivity of a certain product was calculated based on carbon efficiency, as reported previously [10].

2.3. Catalyst characterization

The X-ray powder diffraction (XRD) spectra of samples were obtained on a Rigaku D/MAX-IIIA X-ray diffractometer with CuKα ($\lambda = 0.15418$ nm). The BET surface area of the sample was obtained by N_2 adsorption at −196 °C on a Micromeritics ASAP 2020 apparatus.

2.4. DRIFTS

CO adsorption was studied using a Nicolet 6700 FT-IR spectrometer equipped with a DRIFT cell with CaF_2 windows. The sample in the cell was pretreated in 10% H_2/N_2 at 400 °C for 2 h, and then the temperature was dropped to 30 °C. After the cell was outgassed in vacuum to $<10^{-3}$ Pa, the background was scanned. After CO was introduced for 80 min ($p_{co} = 8.0 \times 10^3$ Pa), the IR spectrum of CO adsorbed on the catalyst was recorded. Then the 10% H_2/N_2 was introduced again, and the IR spectrum of CO adsorbed was recorded as a function of time. The spectral resolution was 4 cm^{-1} and the number of scans was 64.

3. Results and discussion

3.1. CO hydrogenation

The effect of Fe promoter on the catalytic properties of Rh–Mn–Li/SiO_2 catalyst in CO hydrogenation is shown in Table 1. As observed, the CO conversion and yield of C_2^+ oxygenates increase first with the Fe loading, then reach a maximum at Fe amount of ca. 0.1 wt.%, and decrease when the Fe addition exceeded 0.1 wt.%. Interestingly, the selectivities of CH_4 and methanol do not change obviously as the Fe loading was below 0.1 wt.%, but they increase suddenly when the addition of Fe reached 0.5 wt.%. On the other hand, it is found that the selectivity of ethanol decreases when 0.05 wt.% Fe was added into Rh–Mn–Li/SiO_2 catalyst. However, with the further increase of Fe content, the electivity of ethanol increases notably and the selectivity of acetaldehyde decreases.

Thus, it can be seen that the addition of low content of Fe (≤ 0.1 wt.%) can improve the activity and yield of C_2^+ oxygenates; but high Fe loading (>0.1 wt.%) decreases the CO conversion and promotes hydrogenation of CO to form CH_4 and methanol. The increase of ethanol selectivity with the increasing Fe content over the Rh–Mn–Li–Fe/SiO_2 catalysts may be caused by the increased acetaldehyde hydrogenation, which was also proved by other reports [15,16].

3.2. Textural characterization

XRD patterns (not shown) of support and the corresponding catalysts show no crystalline phases, indicating that the SiO_2 is XRD-amorphous and the metal particles are highly dispersed on the SiO_2 support due to the small content. The similar BET surface areas (~15 m^2/g) are obtained on all the samples.

3.3. DRIFTS study

3.3.1. CO adsorption on the catalysts

The FT-IR spectra of the in situ reduced catalysts with different amounts of Fe after CO adsorption at 30 °C for 80 min are compared in Fig. 1. It can be seen that the IR spectrum is mainly composed of a band at ~2067 cm^{-1} and a doublet at ~2100 and ~2030 cm^{-1}, which can be attributed to linearly adsorbed CO [CO(l)] and dicarbonyl $Rh^+(CO)_2$ [CO(gdc)], respectively [17–19]. It is widely accepted that the CO(l) is formed on the Rh^0 sites, and CO(gdc) species is on the Rh^+ sites which may be highly dispersed [20,21]. As the Fe loading increases, the intensities of CO(l) and CO(gdc) decrease, and the degree of decrease of CO(l) is larger than that of CO(gdc), which can be reflected clearly by the peak area ratio of CO(l) versus CO(gdc) (CO(l)/CO(gdc)) shown in Table 2.

Based on the above results, it can be inferred that the addition of Fe can decrease the Rh coverage and impede the CO adsorption, which is in line with the results reported by Mo et al. [13] and Yin et al. [7]. By comparing the degree of decrease of CO(gdc) with that of CO(l), it is suggested that CO(gdc) is more stable on the Fe-promoted catalyst. Similarly, Haider et al. [1] have also reported that CO(gdc) is more thermally stable on the Fe-promoted catalyst.

3.3.2. The desorption behavior of adsorbed CO in H_2 flow

Fig. 2 shows the IR spectra of adsorbed species on the in situ reduced catalysts by H_2/N_2 flow flushed into the cell after CO adsorbed at 30 °C. For all the catalysts, the intensity of CO(l) decreases rapidly at first. As the time increases, the intensity of CO(gdc) decreases, along with the new bands at around 2055 cm^{-1} and 1800 cm^{-1} raising slowly. The 1800 cm^{-1} band can be assigned to bridge bonded CO [CO(b)] [17] and the 2055 cm^{-1} band can be attributed to rhodium carbonyl hydride species [H–Rh–CO] (i.e., re-formation of metallic Rh from isolated Rh^+) [21–23]. In related work, the researches by Solymosi [21] and Guglielminotti [6] also gave IR spectra similar to our observation for the changes of CO adsorption in the presence of H_2, suggesting that the absorbed CO can be changed in the presence of H_2 at room temperature. By comparing the time required for the complete transformation of CO(gdc) over different catalysts, it can be inferred that the increased amount of Fe could promote the rate of transformation.

Moreover, it can be seen from Fig. 2 and Table 2 that the peak area ratio of the final H–Rh–CO and CO(b) species versus original CO(gdc) on the catalysts decreases in the order: Rh–Mn–Li/SiO_2 > Rh–Mn–Li–0.05Fe/SiO_2 > Rh–Mn–Li–0.1Fe/SiO_2. This result suggests that the CO(gdc) species can be changed in two different modes: (a) desorbed associatively, (b) transformed into H–Rh–CO and CO(b), and the increase of Fe amount could enhance the CO(gdc) desorption rather than transformation. In addition, it can also be seen from Table 2 that the peak area ratios of H–Rh–CO versus CO(b) species on the various catalysts at the final time were almost the same, which indicated that the percentage of H–Rh–CO transformed from the CO(gdc) species over the different catalysts was almost consistent.
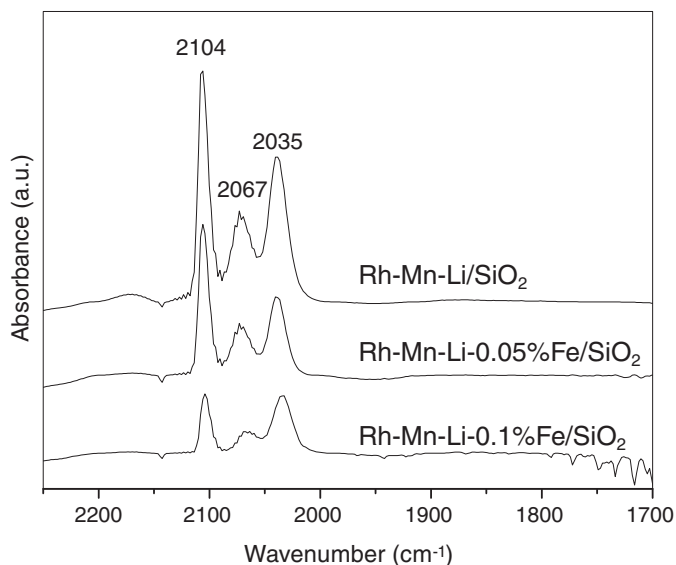
Table 1
Effect of Fe loading on performance of CO hydrogenation over Rh–Mn–Li–Fe/SiO_2 catalysts.

Fe (%)	CO conv. (C%)	Selectivity of products (C%)							STY(C_2^+ Oxy) (g/(kg·h))[a]
		CO_2	CH_4	MeOH	AcH	EtOH	C_2^+ Oxy[b]	C_2^+ HC[c]	
0	18.9	1.1	12.1	2.3	25.4	27.1	54.3	30.2	309.1
0.05	24.4	1.2	12.4	0	42.7	18.9	63.2	23.2	451.8
0.1	28.2	1.4	11.7	0.61	32.8	22.9	58.2	28.1	491.0
0.5	14.8	5.3	30.2	12.7	5.6	35.1	40.7	11.1	201.5

Reaction conditions: 300 °C, 3 MPa, S.V. = 10,000 mL/(g·h), V(H_2)/V(CO) = 2, data taken after 15 h when steady state was reached. Experimental error: ±5%.
[a] STY(C_2^+ Oxy): Space time yield of C_2^+ Oxy
[b] C_2^+ Oxy denotes oxygenates containing two and more carbon atoms.
[c] C_2^+ HC denotes hydrocarbons containing two and more carbon atoms.

Fig. 1. The infrared spectra after CO adsorption on the different catalysts at 30 °C for 80 min.

Based on the above discussion, it is proposed that the different catalytic performances of the various catalysts might be related to the desorption/transformation behavior of CO(gdc) species in the reaction. Considering the synergy between Rh and Fe and enhanced hydrogenation ability of Fe reported before [6,15,16], it is conceivable that the addition of Fe promotes the hydrogenation process in the presence of H_2, further increases the desorption/transformation rate of CO(gdc) species, and the increased desorption/transformation rate can promote the CO conversion. Meanwhile, the decreased ratio of acetaldehyde/ethanol (AcH/EtOH) over the Fe-containing catalysts with the increased Fe amount also suggests that Fe enhances hydrogenation ability and boosts the hydrogenation of AcH to EtOH, which is consistent with the conclusion drawn by Mo et al. [13]. Moreover, considering the fact that the H–Rh–CO species formed from CO(gdc) species during CO hydrogenation might be the intermediate for the synthesis of C_2 oxygenate [20,21,24], the inhibition of the formation of H–Rh–CO species by the addition of Fe can explain the decrease of C_2^+ oxygenate selectivity caused by the increase of Fe content.

Based on the IR description and the catalytic performance of catalysts for CO hydrogenation, it is conceivable that the catalytic activity is determined by both total CO adsorption and desorption/transformation rate of CO(gdc): when the desorption/transformation rate of CO(gdc) dominates at the low values of Fe loading (≤ 0.1 wt.%), an increment of desorption/transformation rate is favorable to the

Table 2
The ratio of peak areas of IR bands for the adsorbed CO species [a].

Ratio	Catalyst		
	Rh–Mn–Li/ SiO₂	Rh–Mn–Li–0.05Fe/ SiO₂	Rh–Mn–Li–0.1Fe/ SiO₂
CO(l)/CO(gdc) [b]	0.32	0.30	0.25
[H–Rh–CO + CO(b)]/ CO(gdc) [c]	1.92	1.08	0.48
H–Rh–CO/CO(b) [d]	0.74	0.76	0.77

[a] The calculated data was based on the peak area of IR bands shown in Figs. 1 and 2; Experimental error: ±5%.
[b] CO(l)/CO(gdc) denotes the peak area ratio of CO(l) versus CO(gdc) in Fig. 1.
[c] [H–Rh–CO + CO(b)]/CO(gdc) denotes the peak area ratio of the final H–Rh–CO and CO(b) species versus original CO(gdc) in Fig. 2.
[d] H–Rh–CO/CO(b) denotes the peak area ratio of H–Rh–CO versus CO(b) over different catalysts at the final time in Fig. 2.
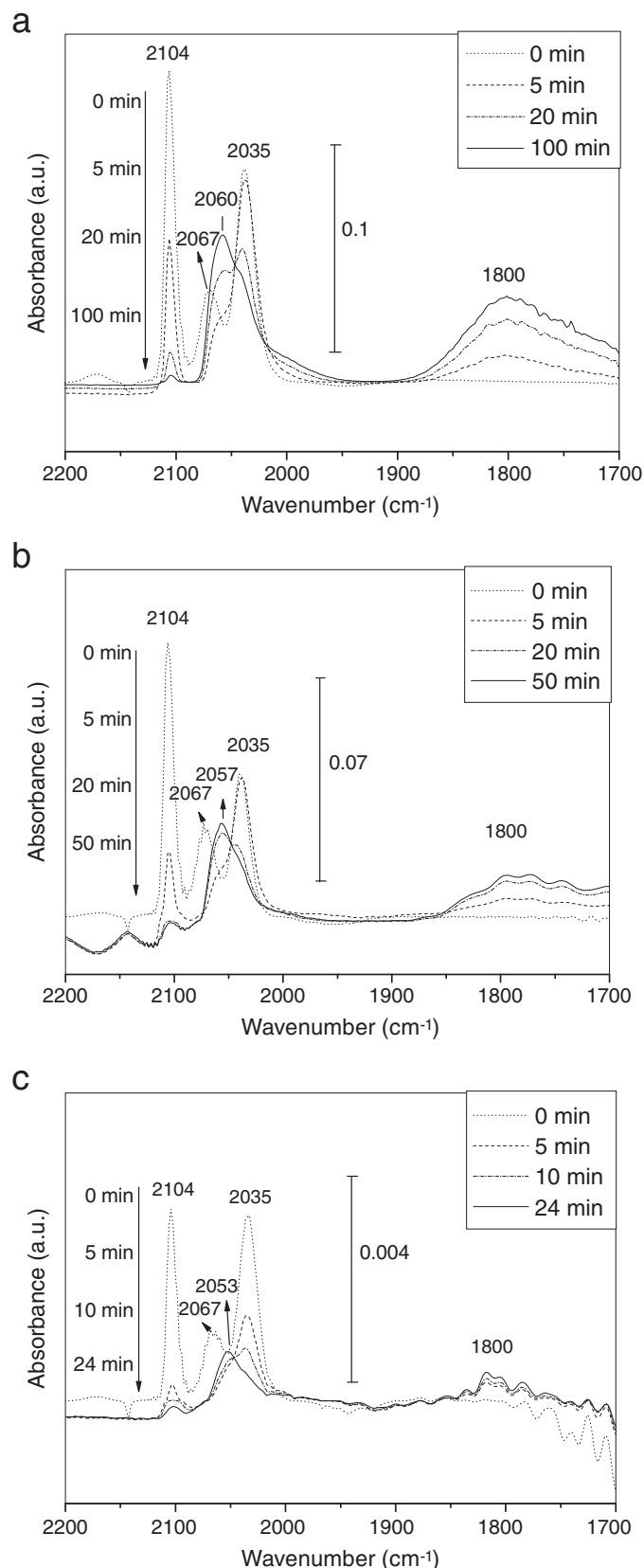

Fig. 2. The infrared spectra after CO adsorption at 30 °C for 80 min followed by flushing with 10% H_2/N_2 (time = 0, start of H_2/N_2 flushing): a) Rh–Mn–Li/SiO₂, b) Rh–Mn–Li–0.05%Fe/SiO₂, c) Rh–Mn–Li–0.1%Fe/SiO₂.

increase of CO conversion; however, the CO conversion decreases due to the serious inhibition of CO adsorption caused by decreased Rh coverage at the high values of Fe (>0.1 wt.%).

4. Conclusions

The effects of Fe promoter on the catalytic properties of Rh–Mn–Li/SiO$_2$ catalysts for the synthesis of C$_2$ oxygenates from syngas were investigated. The results showed that the addition of Fe could improve the CO conversion and yield of C$_2^+$ oxygenates when the doping amount was very low (≤ 0.1 wt.%); and high amount of Fe addition (>0.1 wt.%) would reverse this effect.

The effects of Fe doping for CO adsorption and hydrogenation were investigated using DRIFTS at atmospheric pressure. It was found that the desorption/transformation behavior of adsorbed CO was different with the Fe amount. With the increase of Fe amount, the desorption/transformation rate of CO(gdc) could increase; however, it also decreased the total CO adsorption because Rh particles would be covered by the superfluous amount of Fe. When the positive effect of increasing desorption/transformation rate of CO(gdc) dominates at the low Fe loadings (≤ 0.1 wt.%), the CO conversion increases; however, the CO conversion decreases due to the inevitable decrease of CO adsorption at the high Fe amount (>0.1 wt.%). On the other hand, the decrease in selectivity toward C$_2^+$ oxygenates along with the increase of Fe loading is attributed to the depressing of the transformation of CO(gdc) into H–Rh–CO.

Acknowledgment

References

[1] M.A. Haider, M.R. Gogate, R.J. Davis, Journal of Catalysis 261 (2009) 9–16.
[2] S.S.C. Chuang, R.W. Stevens Jr., R. Khatri, Topics in Catalysis 32 (2005) 225–232.
[3] J.P. Hindermann, G.J. Hutchings, A. Kiennemann, Catalysis Reviews—Science and Engineering 35 (1993) 1–127.
[4] G. Van der Lee, V. Ponec, Catalysis Reviews—Science and Engineering 29 (1987) 183–185.
[5] J.J. Spivey, A. Egbebi, Chemical Society Reviews 36 (2007) 1514–1528.
[6] E. Guglielminotti, F. Pinna, M. Rigoni, G. Strukul, L. Zanderighi, Journal of Molecular Catalysis A: Chemical 103 (1995) 105–116.
[7] H.M. Yin, Y.J. Ding, H.Y. Luo, H.J. Zhu, D.P. He, J.M. Xiong, L.W. Lin, Applied Catalysis A: General 243 (2003) 155–164.
[8] H.Y. Luo, P.Z. Lin, S.B. Xie, H.W. Zhou, C.H. Xu, S.Y. Huang, L.W. Lin, D.B. Liang, P.L. Yin, Q. Xin, Journal of Molecular Catalysis A: Chemical 122 (1997) 115–123.
[9] H. Arakawa, T. Fukushima, M. Ichikawa, S. Natsushita, K. Takeuchi, T. Matsuzaki, Y. Sugi, Chemistry Letters (1985) 881–884.
[10] J. Yu, D.S. Mao, L.P. Han, Q.S. Guo, G.Z. Lu, Catalysis Communications 24 (2012) 25–29.
[11] R. Burch, M.J. Hayes, Journal of Catalysis 165 (1997) 249–261.
[12] X. Mo, J. Gao, J.G. Goodwin Jr., Catalysis Today 147 (2009) 139–149.
[13] X. Mo, J. Gao, N. Umnajikaseam, J.G. Goodwin Jr., Journal of Catalysis 267 (2009) 167–176.
[14] J. Gao, X. Mo, J.G. Goodwin Jr., Journal of Catalysis 268 (2009) 142–149.
[15] R. Burch, M.I. Petch, Applied Catalysis A: General 88 (1992) 39–60.
[16] R. Burch, M.I. Petch, Applied Catalysis A: General 88 (1992) 61–76.
[17] A.C. Yang, C.W. Garland, Journal of Physical Chemistry 61 (1957) 1504–1512.
[18] F. Solymosi, M. Pasztor, Journal of Physical Chemistry 89 (1985) 4789–4793.
[19] J. Gao, X. Mo, A.C. Chien, W. Torres, J.G. Goodwin Jr., Journal of Catalysis 262 (2009) 119–126.
[20] P. Basu, D. Panayotov, J.T. Yates, Journal of Physical Chemistry 91 (1987) 3133–3136.
[21] F. Solymosi, M. Pásztor, Journal of Physical Chemistry 90 (1986) 5312–5317.
[22] F. Solymosi, A. Erdöhelyi, M. Kocsis, Journal of Catalysis 65 (1980) 428–436.
[23] M.L. McKee, C.H. Dai, S.D. Worley, Journal of Physical Chemistry 92 (1988) 1056–1059.
[24] F. Solymosi, I. Tombacz, M. Kocsis, Journal of Catalysis 75 (1982) 78–93.